

# Cortical network modeling: Analytical methods for firing rates and some properties of networks of LIF neurons

Henry C. Tuckwell

*Max Planck Institute for Mathematics in the Sciences, Inselstr. 22, Leipzig D-04103, Germany*

---

## Abstract

The circuitry of cortical networks involves interacting populations of excitatory (E) and inhibitory (I) neurons whose relationships are now known to a large extent. Inputs to E- and I-cells may have their origins in remote or local cortical areas. We consider a rudimentary model involving E- and I-cells. One of our goals is to test an analytic approach to finding firing rates in neural networks without using a diffusion approximation and to this end we consider in detail networks of excitatory neurons with leaky integrate-and-fire (LIF) dynamics. A simple measure of synchronization, denoted by  $S_q$ , where  $q$  is between 0 and 100 is introduced. Fully connected E-networks have a large tendency to become dominated by synchronously firing groups of cells, except when inputs are relatively weak. We observed random or asynchronous firing in such networks with diverse sets of parameter values. When such firing patterns were found, the analytical approach was often able to accurately predict average neuronal firing rates. We also considered several properties of E–E networks, distinguishing several kinds of firing pattern. Included were those with silences before or after periods of intense activity or with periodic synchronization. We investigated the occurrence of synchronized firing with respect to changes in the internal excitatory postsynaptic potential (EPSP) magnitude in a network of 100 neurons with fixed values of the remaining parameters. When the internal EPSP size was less than a certain value, synchronization was absent. The amount of synchronization then increased slowly as the EPSP amplitude increased until at a particular EPSP size the amount of synchronization abruptly increased, with  $S_5$  attaining the maximum value of 100%. We also found network frequency transfer characteristics for various network sizes and found a linear dependence of firing frequency over wide ranges of the external afferent frequency, with non-linear effects at lower input frequencies. The theory may also be applied to sparsely connected networks, whose firing behaviour was found to change abruptly as the probability of a connection passed through a critical value. The analytical method was also found to be useful for a feed-forward excitatory network and a network of excitatory and inhibitory neurons.

© 2006 Elsevier Ltd. All rights reserved.

*Keywords:* Neural networks; Cortical networks; LIF model; Random activity; Analytical methods; Synchronization

---

## 1. Introduction

The electrophysiological activity and properties of cortical neuronal networks have been of much interest for the previous 100 years (Sherrington, 1906). As detailed knowledge of neurophysiology and neuroanatomy has grown since about 1950, mathematical models have been devised to try to explain the more salient features of the spread of neuronal activity including such phenomena as travelling waves and population oscillations (Bazhenov et al.,

2005; Gerstner, 2000; Liley et al., 1999; Rulkov et al., 2004; Tuckwell and Miura, 1978). However, since the appearance of Hebb's fundamental work (Hebb, 1949) on neural assemblies and synaptic modification, much attention has been directed to the actual patterns of spiking activity of cortical and other neuronal networks (Abeles, 1991; Amit, 1989; Gerstner and Kistler, 2002). One aspect of spiking activity within cortical networks, synchronization, has been hypothesized to play an important role in information processing (Konig, 1994; Konig et al., 1996a; Singer, 1993, 1999). An interesting empirical observation is that, at least in visual cortex, synchronization concomitant with oscillation tended to be found for neurons

---

*E-mail address:* [tuckwell@mis.mpg.de](mailto:tuckwell@mis.mpg.de)

separated by large distances but not over smaller distances (Konig et al., 1996a), indicating that in the latter instances the synchronization is due to common inputs. Synchronization has also been posited as playing a key role in certain memory processes (Axmacher et al., 2006). However, whereas some have claimed that synchronization is useful within the cortex to group together cells involved in a common task, it is not certain if it has real significance (Tiesinga and José, 2000) as it may just be an incidental property of active networks.

In order to analyze theoretically the spiking behaviour of cortical and other neuronal networks, a variety of models for single neurons has been employed. At the level of greatest simplicity are those which represent neurons as zero–one elements (Hopfield, 1982). The inclusion of some physiological properties of real neurons is effected by using the leaky integrate-and-fire (LIF) model in various forms (Abbott and Van Vreeswijk, 1993; Amit and Brunel, 1997a; Brunel, 2003; Brunel et al., 2001; Brunel and Hakim, 1999; Brunel and Hansel, 2006; Deco and Rolls, 2005; Hansel and Mato, 2003; Knight, 1972; Neltner et al., 2000; Van Rossum et al., 2002; Van Vreeswijk and Abbott, 1993). Such relatively simple models have the advantage that their use does not require much computer memory so that large populations are fairly easily studied. More complex and hence more realistic models which incorporate not only many ion channels but also the spatial extent of a neuron's soma-dendritic surface (Destexhe and Paré, 1999; Destexhe et al., 2001) have also been employed (Bush and Sejnowski, 1995; Liley et al., 1999), but have the disadvantage of requiring much computer memory and a large number of parameters. As alluded to above, one may also adopt a continuum approach where the discrete nature of neural populations is smoothed out so that the spiking of individual neurons is not distinguished (Beurle, 1956; Bresloff and Coombes, 1998; Gerstner, 2000; Tuckwell, 1998) and a “map-based” approach where the dynamics of neuronal activity is summarized in a firing rate function (Tuckwell, 1998; Rulkov et al., 2004). However, with the emphasis on the role of spike-timing in theories of cognitive processes (Axmacher et al., 2006; Konig et al., 1996b; Perez-Orive et al., 2004), it is likely that the models of cortical networks that distinguish individual neurons and their spike occurrences in both space and time will prove more useful in the understanding of central nervous system function.

Investigations of neural networks often rely on simulations, but it is also desirable to have analytical results. The latter have been achieved in early work concerning oscillators (Abbott and Van Vreeswijk, 1993) and more recently useful results have been obtained for networks of LIF model neurons using diffusion approximations (Amit and Brunel, 1997a,b; Brunel, 2000; Brunel et al., 2001). For example, methods for analyzing the stability of asynchronous states using a diffusion approach have been given in Amit and Brunel (1997b) and Brunel (2000). Deng et al. (2004) have obtained theoretical results on the

stability of synchronized states in a more general framework.

However, diffusion models are deficient in many parameter ranges (Tuckwell and Cope, 1980) and our aim in this article is to demonstrate that an analytical approach is sometimes useful in determining firing rates in some LIF networks when a diffusion approximation is not made. Such an approach may be extended to networks composed of generalized Hodgkin–Huxley neurons (Tuckwell and Feng, 2006). To demonstrate the methods we consider the following three LIF networks: (i) a fully connected network of excitatory neurons (ii) a feed-forward network (Van Rossum et al., 2002) and (iii) a network containing both excitatory and inhibitory elements. We are interested in the conditions under which network elements fire in a random or asynchronous fashion, as opposed to firing synchronously in groups, and in determining some of the parameter dependence of the general network firing characteristics. In particular we examine, in the fully connected case, the effects of changing external afferent frequency, the intra-network EPSP amplitude and the size of the network.

### 1.1. Structure of cortical neuronal networks

The anatomical details of neuronal connections in the mammalian cerebral cortex are still being determined, but recently there have been published comprehensive schemes involving excitatory and inhibitory cells in various layers along with external thalamic inputs (Douglas and Martin, 2004). Cortical circuits involve excitatory (spiny cells) and smooth inhibitory neurons with numbers in the ratio of about 4 to 1. Inhibitory cells are usually fast spiking interneurons, with only local connections, which may be predominantly vertical or horizontal. These cells and their subtypes have quite different anatomical and physiological properties and have different concentrations in the various layers (McCormick et al., 1985). Excitatory cells send their output through both local and long range connections to other parts of cortex or other structures (Binzegger et al., 2005).

An accurate model of a cortical network would ideally take into account the various cell types, some of which were mentioned above, as well as the cortical layer in which a given neuron occurs. The number of neurons under an area of 1 mm<sup>2</sup> of cortex is between 30,000 and 60,000 (Hilgetag and Barbas, 2006) so a reasonable sample would be an area of about 1/10 mm<sup>2</sup> containing about 5000 neurons, of which approximately 4000 are excitatory and 1000 are inhibitory. It is a large computational challenge to incorporate such details within the limits of a model which is not excessively complicated (Bush and Sejnowski, 1995; Grillner et al., 2005; Haeusler and Maass, 2006). Furthermore, the spatial aspects of single neurons can be important (Bush and Sejnowski, 1995) and distributions of synapses are not uniform. For example, in cat parietal cortex a pyramidal cell receives about 20,000 synapses of which about 80% are excitatory, the remainder being inhibitory but

more concentrated towards the soma (Bush and Sejnowski, 1995). The geometry of connections is usually ignored altogether, but simplified connectivity patterns are sometimes assumed. For example, in one approach, excitatory cells synapse with 12 neighbouring excitatory cells and 3 neighbouring inhibitory cells while inhibitory cells act upon 7 neighbouring excitatory cells and no inhibitory cells (Bazhenov et al., 2005). Although inhibitory–inhibitory connections are few in number, they may play an important role (Brunel and Hansel, 2006; Somogyi et al., 1998). Given the complexity of real cortical networks, it is natural to consider simplified models.

### 1.1.1. Simplified cortical network models

For spike generation we choose LIF models similar to those employed by Amit and Brunel (1997b) and Brunel (2000). Suppose there are  $n_E$  excitatory cells and  $n_I$  inhibitory cells in total. Let the potentials (depolarizations) of the excitatory cells be  $V_j^E$  where  $j = 1, \dots, n_E$  and those of the inhibitory cells be  $V_i^I$ , where  $i = 1, \dots, n_I$ . Let  $\tau_E$  and  $\tau_I$  be the corresponding time constants and let the connection matrices from E to E, I to E, E to I and I to I have elements  $a_{kj}^{EE}$ ,  $a_{ij}^{IE}$ ,  $a_{ki}^{EI}$  and  $a_{li}^{II}$ , respectively, where all these matrix elements, here assumed to be non-negative, are random variables whose probability distributions depend on the distances between the various kinds of individual neurons,  $d_{kj}^{EE}$ ,  $d_{ij}^{IE}$ ,  $d_{ki}^{EI}$  and  $d_{li}^{II}$ . The corresponding times for transmission of impulses are  $t_{kj}^{EE}$ ,  $t_{ij}^{IE}$ ,  $t_{ki}^{EI}$  and  $t_{li}^{II}$ . The spike trains of the excitatory neurons are the point processes  $N_j^E$  and those of the inhibitory neurons are  $N_i^I$ . External inputs are designated  $N_j^{E,ext}$  and  $N_i^{I,ext}$ , to E- and I-cells respectively with corresponding EPSP and IPSP amplitudes  $\epsilon_j^{E,ext}$  and  $\epsilon_i^{I,ext}$ . The equations describing the excitatory cells are

$$dV_j^E = -\frac{V_j^E}{\tau_E} dt + \epsilon_j^{E,ext} dN_j^{E,ext} + \sum_{k=1}^{n_E} a_{kj}^{EE} dN_k^E(t - t_{kj}^{EE}) - \sum_{l=1}^{n_I} a_{lj}^{IE} dN_l^I(t - t_{lj}^{IE}), \quad V_j^E < \theta_E$$

and the equations for the I-cells are

$$dV_i^I = -\frac{V_i^I}{\tau_I} dt + \epsilon_i^{I,ext} dN_i^{I,ext} + \sum_{k=1}^{n_E} a_{ki}^{EI} dN_k^E(t - t_{ki}^{EI}) - \sum_{l=1}^{n_I} a_{li}^{II} dN_l^I(t - t_{li}^{II}), \quad V_i^I < \theta_I,$$

where  $\theta_E$  and  $\theta_I$  are the thresholds of the two populations. After a neuron's depolarization reaches or exceeds threshold, it is reset to resting level as it emits a spike to target cells. A refractory period may ensue. Along with initial conditions, the above stochastic equations completely describe the activity in the model cortical network. Now as we wish to explore an analytical theory in a simple case first, we restrict our attention to networks containing only excitatory elements. Such networks may arise in the cortex if inhibition is nullified, as for example by applying the GABA-blocker bicuculline.

### 1.1.2. Networks of excitatory LIF neurons

Although, as described above, neuronal populations in the cerebral cortex and other central nervous system structures invariably contain both excitatory neurons and inhibitory neurons, many theoretical studies have examined networks composed of model neurons which only make excitatory synaptic contact with each other or there may be only inhibitory neurons (Brunel and Hakim, 1999; Brunel and Hansel, 2006). We begin by considering a network of purely excitatory elements. We are interested in determining in a systematic fashion the manner in which the activity in such networks depends on various parameters. In the case where the elements in the network are LIF neurons, we may summarize the dynamical properties of the model as follows:

- (i) The number of neurons is  $n$ .
- (ii) The connection strength from neuron  $j$  to neuron  $k$  is  $a_{jk}$ ,  $j = 1, \dots, n$ ;  $k = 1, \dots, n$ .  
Unless otherwise stated we put  $a_{jj} = 0$ ,  $j = 1, \dots, n$ . These quantities are dimensionless.
- (iii) Neuron  $j$  has a threshold for firing of  $\theta_j$  mV. Unless otherwise stated all thresholds are the same,  $\theta_j = \theta$ .
- (iv) Neuron  $j$  receives external input from a standard Poisson process  $N_j^{ext}$  with rate  $\lambda_j$  per second. Unless otherwise stated all these rates are the same  $\lambda_j = \lambda_{ext}$ .
- (v) When neuron  $j$  receives an external excitatory input, its membrane potential is depolarized by  $\epsilon_j^{ext}$  mV. Unless otherwise stated all these are the same,  $\epsilon_j^{ext} = \epsilon_{ext}$ .
- (vi) When neuron  $j$  within the network fires, if it elicits an EPSP in neuron  $k$  then it has magnitude  $\epsilon_{jk}$ . Usually we put  $\epsilon_{jk} = \epsilon_{int}$ .
- (vii) The membrane potential (depolarization from resting level, 0) at time  $t$  of neuron  $j$  is  $V_j(t)$ .
- (viii) The initial value of  $V_j(t)$  is uniformly randomly distributed on  $(0, \theta_j)$  or is at resting level, 0.
- (ix) If  $V_j(t)$  exceeds  $\theta_j$ , neuron  $j$  fires an action potential at its target neurons and its potential is reset to rest after a refractory period of  $t_R$  seconds. Usually we put  $t_R = 0$ .
- (x) The time constant of decay of the membrane potential of neuron  $j$  is  $\tau_j$ . Usually we put  $\tau_j = \tau$ , the same for all neurons.

## 2. Methods

### 2.1. Theory of firing rates

There are few analytical results available which describe the activity in neural networks, but see, for example, Amit and Brunel (1997a,b), Brunel (2000) and Brunel et al. (2001) for some of those previously described for diffusion processes. We present a method for estimating the mean interspike interval of neurons in the simple network described in the previous paragraph. For such a network, we may write the following system of  $n$  coupled equations:

$$dV_j(t) = -\frac{V_j(t)}{\tau} dt + \epsilon_{\text{ext}} dN_j^{\text{ext}}(t) + \sum_{k=1}^n a_{kj} \epsilon_{kj} dN_k(t - t_{kj}),$$

$$j = 1, 2, \dots, n, \tag{1}$$

which applies when  $V_j$  is less than threshold  $\theta$ , assumed the same for all neurons. Here  $t_{kj}$  is the time delay for transmission from neuron  $k$  to neuron  $j$ , but we set these delays at zero for the remainder of the article. The term  $dN_k$  gives rise to a delta function in the derivative of  $V_j$  at the spike emission times of neuron  $k$ , so that the depolarization of neuron  $j$  jumps by  $a_{kj}\epsilon_{kj}$  at such times.

If they are identical physiologically, all the neurons in the network fire at about the same mean rate because they all get versions of the same point process input from the other  $n - 1$  cells. Thus, the input frequency in a network of identical neurons each of which receives  $(n - 1)$  inputs is  $(n - 1)$  times the output frequency of each cell. Assuming that the common rate is  $\lambda$  spikes per second, then each neuron acts like one whose activity is described for subthreshold voltages by

$$dV = -\frac{V}{\tau} dt + \epsilon_{\text{ext}} dN^{\text{ext}}(t) + \epsilon_{\text{int}} dN(t), \tag{2}$$

where  $N$  is a counting process, assumed to be approximately Poisson, with rate parameter  $(n - 1)\lambda$ , and  $\epsilon_{\text{int}}$  is the EPSP amplitude within the network. We have also assumed that  $a_{jk} = 1$  for  $j \neq k$ . We then have the following analytical result (Tuckwell, 1975). Here  $F(v)$  is the mean time for the voltage to attain threshold  $\theta$  for an initial value  $V(0) = v$ , so that the mean time to reach threshold from rest is given by  $F(0)$ .

If  $\frac{1}{\lambda}$  is the mean time interval between spikes in a neuron of the network described above, then it may be estimated by solving the differential-difference equation

$$-\frac{v}{\tau} \frac{dF}{dv} + (n - 1)\lambda[F(v + \epsilon_{\text{int}}) - F(v)] + \lambda_{\text{ext}}[F(v + \epsilon_{\text{ext}}) - F(v)] = -1, \tag{3}$$

for  $v < \theta$ , with boundary conditions  $F(v) = 0$ ,  $v \geq 0$  and  $F(0^+) = \frac{1}{\lambda}$ .

One may also incorporate a refractory period in this approach. Solving Eq. (3) enables one to estimate the rate of firing in the network, assuming that there is not a great deal of synchrony or roughly simultaneous firing of large groups of neurons. We will call a result obtained by this approach a predicted one versus one from direct simulation of a network. Because it is not straight forward to solve (3) using algebraic methods (Tuckwell, 1975) we find the solution by finding self-consistent rates from solutions of (2). Simulation procedures are discussed briefly in the appendix.

### 3. Results

#### 3.1. Sustained random firing

Many sets of parameters for purely excitatory networks result in considerable synchronization as the population breaks up into a few or many coordinated groups. These patterns are very stable once formed. However, there are also several sets of parameters for which the network shows

no signs of splitting into such groups and a sustained pattern of random or ‘‘asynchronous’’ firing occurs, at least over reasonably long time periods.

It is clear that as a rough guide, if a large degree of synchrony is to be avoided the product  $n\epsilon_{\text{int}}$  must be small relative to  $\theta$ , so that if a substantial subset of cells does fire at about the same time, it will not induce a very large depolarization in many other cells in the population. Such conditions promote the dominance of the random external Poisson input, for which we note that there is no threshold frequency for firing. For example, the following parameter values led to random firing in a network of  $n = 2$  neurons:  $\theta = 15$  mV,  $\tau = 20$  ms,  $\lambda_{\text{ext}} = 750$  Hz,  $\epsilon_{\text{ext}} = 1.5$  mV,  $\epsilon_{\text{int}} = 3.0$  mV,  $a_{jk} = 1$ ,  $j \neq k$  and  $a_{jj} = 0$ ,  $V_j(0) = 0$  for all  $j$ , and  $t_R = 0$ . The results of network simulation and theory are shown for this example in the first row of Table 1. A sequence of networks of increasing size was then investigated by simulation and theory and the corresponding results obtained are also shown in Table 1 sometimes with different values of some of the parameters, as indicated in columns 2–4.

In order to make the term ‘‘synchronous’’ more precise, it is necessary to define synchronous firing in terms of measurable quantities. Often the definition involves correlation or coherence (Konig, 1994) or related quantities (Samonds and Bonds, 2004), but here we pursue a simpler approach and introduce the following quantities which are useful when the population size is large enough (e.g. greater than 50). Let  $S_q$  be the percentage of the number of epochs of the ‘‘experiment’’ when there was any firing at all, during which a fraction greater than  $q$  of the population of neurons participated in the firing. Thus,  $S_5 = 10\%$  means that of the epochs when at least one neuron fired, then the fraction of epochs during which more than 5% of the population was firing was 0.1. Usually we examine the quantities  $S_5, S_{10}, S_{15}$  and  $S_{20}$  to assess the degree of synchronization. If all these quantities are zero (for large enough  $n$ ) then the firing will be called asynchronous. Note that from a plot of number of neurons firing versus time period, if no more than  $r\%$  of the neurons ever fired simultaneously, it can be deduced that  $S_r = 0$ .

An example of sustained asynchronous firing with 50 neurons is illustrated in Fig. 1. Here the synchronization measure  $S_4 = 0$  as there were never more than two neurons

Table 1  
Results and predictions for networks of various sizes

| Network size, $n$ | $\epsilon_{\text{ext}}$ | $\lambda_{\text{ext}}$ | $\epsilon_{\text{int}}$ | Network frequency | Predicted frequency | Single neuron | Disconn. net |
|-------------------|-------------------------|------------------------|-------------------------|-------------------|---------------------|---------------|--------------|
| 2                 | 1.5                     | 750                    | 3.0                     | 60.3              | 59.5                | 47.6          | 47.2         |
| 3                 | 1.0                     | 750                    | 3.0                     | 35.3              | 36.5                | 20.3          | 22.2         |
| 4                 | 1.0                     | 750                    | 1.5                     | 31.7              | 33.3                | 20.3          | 20.7         |
| 5                 | 1.0                     | 750                    | 1.5                     | 35.8              | 36.4                | 20.3          | 20.7         |
| 10                | 1.0                     | 750                    | 0.75                    | 42.4              | 42.0                | 20.3          | 20.9         |
| 20                | 1.0                     | 600                    | 0.4                     | 24.4              | 24.4                | 9.5           | 10.5         |
| 50                | 1.0                     | 500                    | 0.2                     | 7.0               | 8.4                 | 3.3           | 3.8          |
| 100               | 1.0                     | 500                    | 0.05                    | 6.5               | 6.4                 | 3.3           | 4.6          |
| 500               | 1.0                     | 500                    | 0.01                    | 7.5               | 7.6                 | 3.3           | 4.6          |
| 1000              | 1.0                     | 500                    | 0.0075                  | 12.4              | 11.3                | 3.3           | 4.5          |

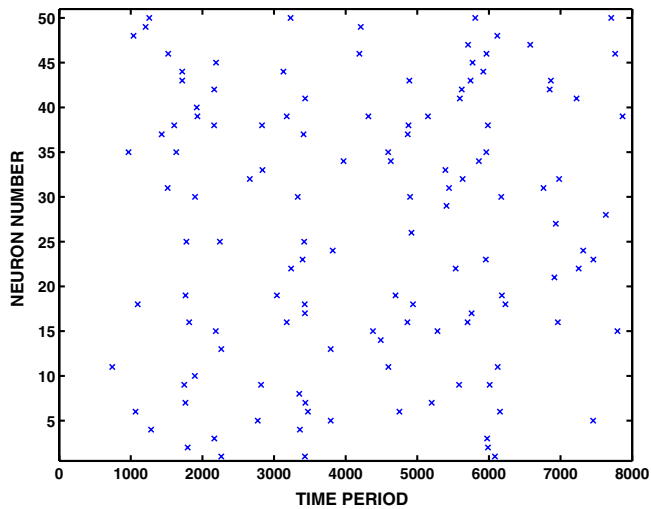


Fig. 1. Sustained random spiking in a fully connected network of  $n = 50$  excitatory neurons with external Poisson input. The parameters are as follows.  $\theta = 15$  mV,  $\tau = 20$  ms,  $\lambda_{\text{ext}} = 500$  per s,  $\epsilon_{\text{ext}} = 1.0$  mV,  $\epsilon_{\text{int}} = 0.15$  mV,  $a_{jk} = 1$ ,  $j \neq k$  and  $a_{jj} = 0$ ,  $V_j(0) = 0$  for all  $j$ ,  $t_R = 0$ . Time step  $\Delta t = 0.00005$  s.

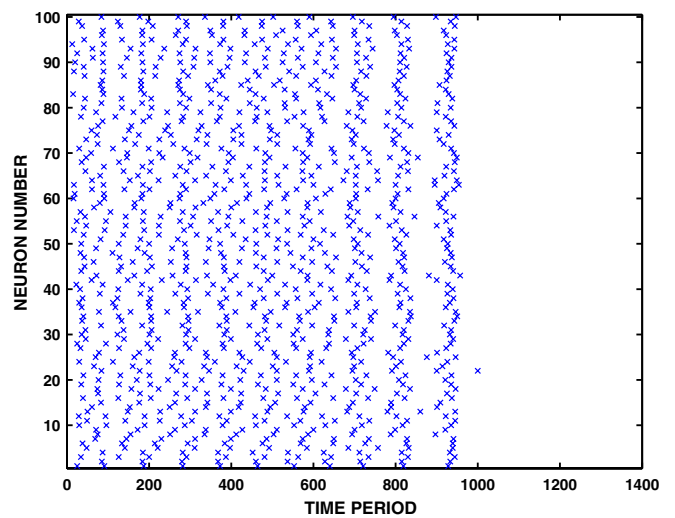


Fig. 2. Spike pattern in a network of 1400 neurons where the activity dies away spontaneously – for parameters see text.

firing simultaneously. All the parameter values are given in the caption of the figure. There is an initial period of settling in, due to the fact that all the neurons were started in the resting state. These initial data were chosen in order to make a more rigorous comparison with the theoretical predictions. The phenomena are however essentially the same if the initial conditions were randomized. The spike rates in the network simulations shown in Table 1 were calculated after the settling in period.

However, it was observed, infrequently, that in some cases an apparently stable random firing pattern was established but that it subsequently died away completely, despite the fact that the external Poisson input was still switched on. This phenomenon, which was unusual, occurred in a network of  $n = 1400$  neurons with the following parameter set:  $\theta = 15$ ,  $\tau = 20$  ms,  $\lambda_{\text{ext}} = 520$  Hz,  $\epsilon_{\text{ext}} = 0.6$  mV,  $\epsilon_{\text{int}} = 0.01$  mV,  $a_{jk} = 1$ ,  $j \neq k$  and  $a_{jj} = 0$ , and  $t_R = 0$ . In this case the initial potentials were randomly distributed from resting value to threshold. The spike raster (reduced) is plotted in Fig. 2 and the corresponding spike frequency plotted versus time period in Fig. 3. Evidently the external input is not strong enough to induce firing when the rates across the network drop randomly to almost zero. On the other hand, it was also observed, infrequently, that a long silent period preceded a building up to firing activity across the network. This is illustrated in Fig. 4, where in a network of 100 neurons, the whole network was silent for about the first 900 epochs, followed by synchronous firing across the population for a few periods, then almost complete silence for 700 periods, then another few periods of synchronous firing. This pattern repeated until about the 4000th period whereafter there was rapid firing in synchronous groups of several neurons. The parameter values for this trial are given in the figure caption.

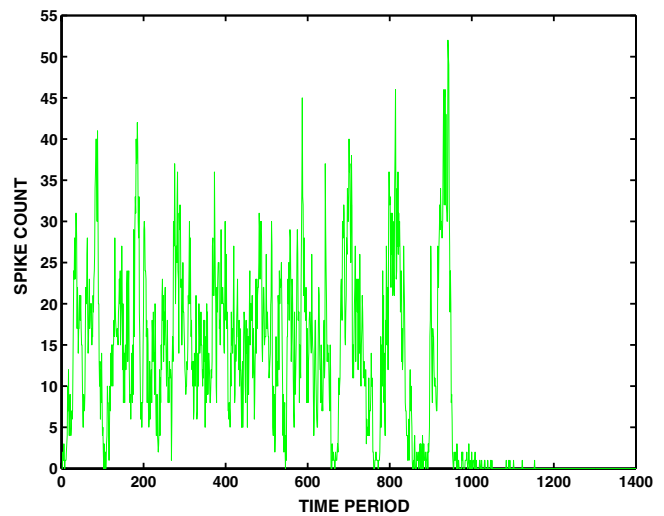


Fig. 3. Spike count versus time for the data of Fig. 2.

It can be seen in the above cases in Table 1 that the agreement between the neuronal firing frequencies obtained by simulation of the network and those predicted from the analytical approach is in all cases very good and in many cases excellent. There is also good agreement between the single neuron frequencies, calculated by the more accurate direct method (see appendix) and the frequencies of the neurons in the network when the connections are removed. Note that in all the examples given in Table 1 the network was firing randomly, without evidence of synchronization. However, even when this was not the case the analytical approach could still give accurate results. For example, with a network of  $n = 1000$  cells and with the same parameters as in Table 1 except  $\epsilon_{\text{int}} = 0.01$  mV, the neuron spiking rate in the simulated network was 33.2 Hz whereas the predicted rate was 32.6 Hz, despite the fact that there was a considerable degree of synchronous firing across the population.

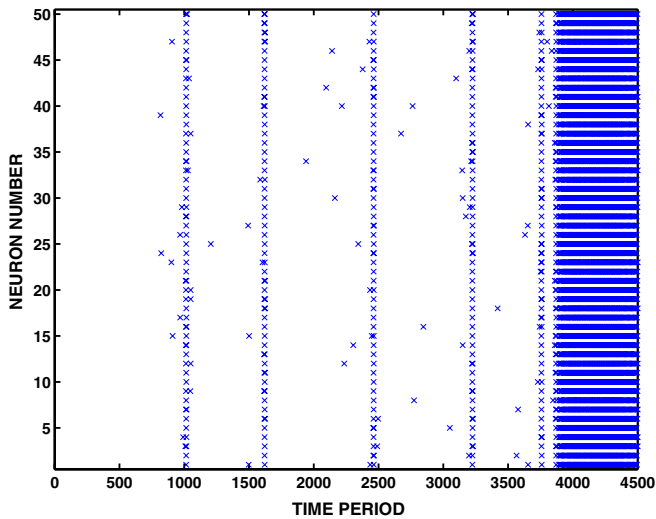


Fig. 4. Periods of silence terminated by short periods of synchronous firing in a network of 100 neurons, followed by rapid firing due to synchronous groups of several neurons. Only the spikes of 50 neurons are shown. The parameters are as follows:  $\theta = 15$ ,  $\tau = 20$  ms,  $\lambda_{\text{ext}} = 500$  Hz,  $\epsilon_{\text{ext}} = 1.0$  mV,  $\epsilon_{\text{int}} = 0.175$  mV,  $a_{jk} = 1$ ,  $j \neq k$  and  $a_{jj} = 0$ ,  $V_f(0) = 0$  for all  $j$ , and  $t_R = 0. \Delta t = 0.00005$ .

### 3.2. Dependence on network size and external frequency

We investigated the dependence of network activity, as measured by mean unit firing rate, on both the afferent frequency, that is the mean rate of arrival of input from external sources, and the size of the network. Recall that in this section the network is fully connected.

#### 3.2.1. Changes in afferent frequency

In order to see how overall network activity in an excitatory network depended on the afferent frequency  $\lambda_{\text{ext}}$ , the latter was systematically varied whilst all other parameters were held fixed for networks of sizes  $n = 50$  and  $n = 100$ . A restricted range of  $\lambda_{\text{ext}}$  was employed in order to keep a fixed value of  $\Delta t = 0.000025$  s. The parameter values are given in the caption of Fig. 5. In addition, the single neuron output frequencies were obtained by two methods: averaging over 1000 trials using the solution of the stochastic Eq. (2) without the synaptic input term from other neurons in the network and the direct simulation method described in the appendix. All single neuron parameters were held the same as in the network simulations, results for the latter being obtained by averaging over 40,000 time periods. The results for the single neuron are shown in the lower (blue)<sup>1</sup> curve of Fig. 5 – this is often called the frequency transfer characteristic for the (model) neuron. It should be recalled here that a refractory period has not been included. The dependence of mean output frequency on mean afferent input frequency is almost linear for the two network sizes considered. Indeed for the range of input fre-

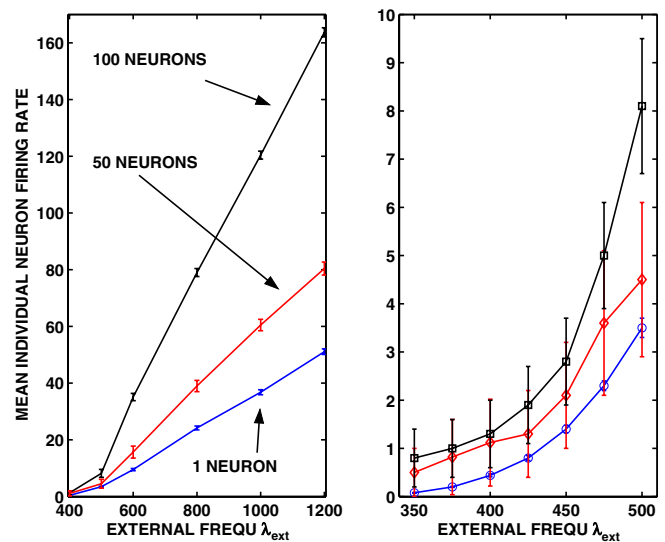


Fig. 5. The changes in mean output frequency of neurons in networks of various sizes as the mean afferent frequency increases. The middle curve is for  $n = 50$  and the uppermost curve is for  $n = 100$ . The right-hand figure shows the low input frequency portion in more detail. All frequencies are in Hz. The error bars denote 95% confidence intervals. The parameters are as follows:  $\theta = 15$  mV,  $\tau = 20$  ms,  $\epsilon_{\text{ext}} = 1.0$  mV,  $\epsilon_{\text{int}} = 0.1$  mV,  $a_{jk} = 1$ ,  $j \neq k$  and  $a_{jj} = 0$ ,  $V_f(0)$  is uniformly distributed on  $(0, \theta)$  for all  $j$  and  $t_R = 0$ .

quencies  $\lambda_{\text{ext}}$  from about 500 to 1200 Hz depicted in Fig. 5, this is the case for networks of  $n = 50$  and  $n = 100$ . However, the curves at mean input frequencies between 350 and 500 Hz are apparently non-linear, as seen in the right-hand portion of Fig. 5. The curve for  $n = 100$  seems to rise more sharply than the other two curves for  $\lambda_{\text{ext}} \geq 450$  Hz, although eventually all three curves are almost linear. Note that these are for stochastic and not deterministic inputs.

#### 3.2.2. Changes in network size

In order to see how network size influenced mean unit activity, the afferent (Poisson) frequencies were held at the three values  $\lambda_{\text{ext}} = 600, 800$  and  $1000$  Hz whilst the network size varied from  $n = 5$  to  $n = 100$ . The remaining parameter values were the same as in the above subsection on variations in afferent frequency. The resulting mean unit frequencies are shown in Fig. 6. Of interest is the fact that when  $n$  is relatively small, the spiking activity is dominated by the (independent) Poisson inputs to the individual cells. This was apparent from the spike rasters which are not shown. In fact for the parameters considered, the non-random component of firing induced by simultaneous excitation of other neurons is not appreciable until the network size is greater than  $n = 50$ –75. It is at about these values of  $n$  that the slopes of the curves of neuron mean spiking frequency start to increase rather sharply due to substantial intra-network contributions to the states of each neuron. The values of  $n$  at which these changes occur will of course depend, *inter alia*, on the internal EPSP amplitude  $\epsilon_{\text{int}}$ .

<sup>1</sup> For interpretation of color in Figs. 5 and 8, the reader is referred to the web version of this article.

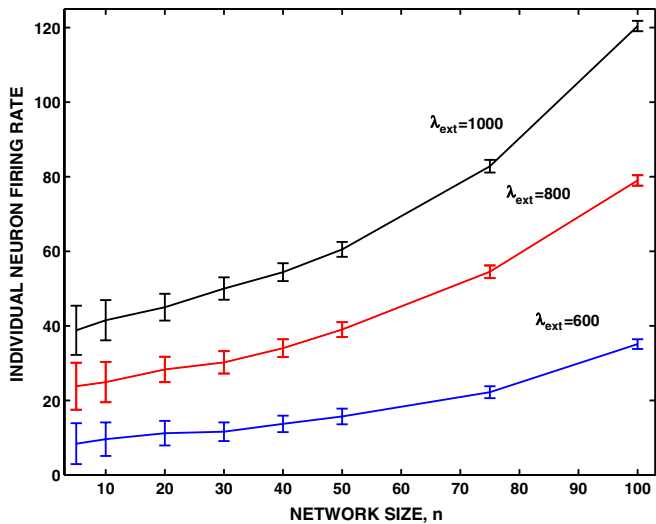


Fig. 6. The changes in output frequency of neurons in networks with various afferent frequencies as the number of network elements  $n$  increases. Error bars are 95% confidence intervals. The parameters are as in the previous figure.

### 3.3. Dependence on internal EPSP size

It is of interest to consider the effects of changing the magnitude of the cell-to-cell excitatory synaptic input in a

network described by Eq. (1) when this quantity is the same for any pair of pre- and post-synaptic cells; that is

$$\epsilon_{ij} = \epsilon_{\text{int}} = \epsilon > 0$$

for all  $i$  and  $j$  except  $i=j$ . We call  $\epsilon$  the internal EPSP amplitude as opposed to  $\epsilon_{\text{ext}}$ . When  $\epsilon$  is zero, or very small, the activity in the network is dominated by the two parameters  $\lambda_{\text{ext}}$  and  $\epsilon_{\text{ext}}$  which when acting alone give rise to purely random firing because each cell is receiving independent random input from outside the network. This is demonstrated in Fig. 7 in the top two frames, where the results of simulations are shown for  $n = 100$  cells. Here  $\epsilon = 0$  (left) and  $\epsilon = 0.05$  (right). The random firing was maintained for 30,000 time steps of 0.00005 s. Much longer trials were performed, up to five times as long, and there was no indication of any non-random firing pattern. In the bottom left frame, where  $\epsilon = 0.09$ , there are vertical bands of simultaneously firing neurons, indicating that synchronization effects are becoming important but are not dominant. In the remaining frame the internal EPSP is  $\epsilon = 0.15$  mV and it can be seen that the firing pattern is dominated by vertical bands of simultaneously firing neurons.

To examine the effect of  $\epsilon$  on the occurrence of various firing patterns, twenty trials were performed as described in the previous paragraph with various values of  $\epsilon$  while all other parameters were held fixed at values as follows:

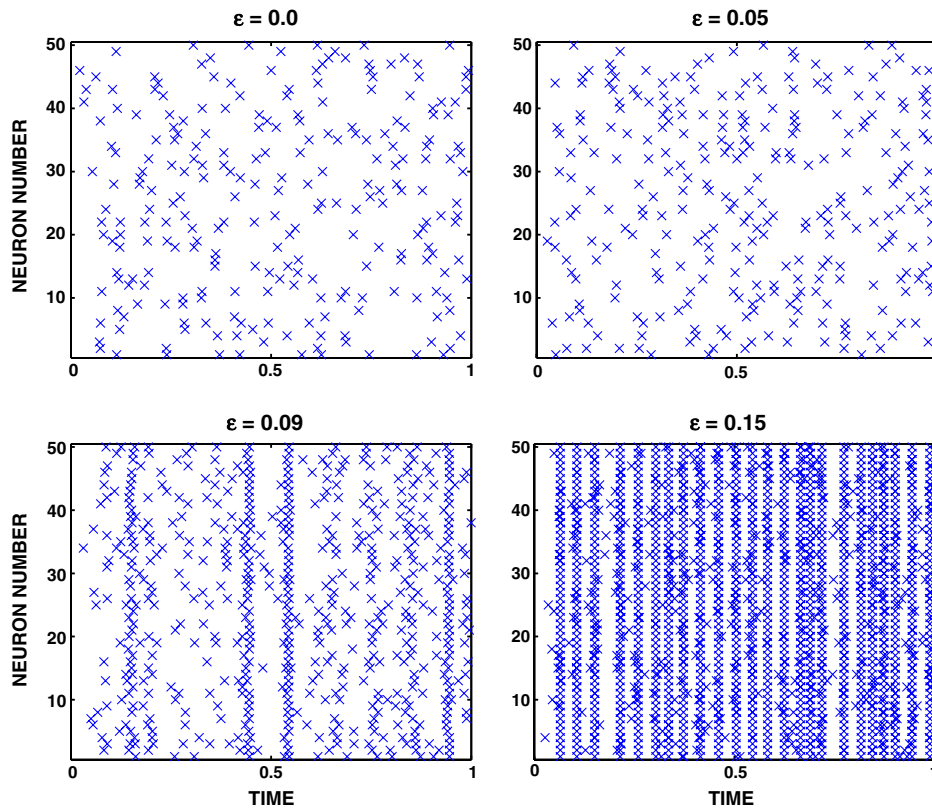


Fig. 7. The changes in the firing patterns in an excitatory network of  $n = 100$  neurons as the network EPSP  $\epsilon$  amplitude changes. Each neuron receives both external Poisson input and input from all the other neurons. The parameters are as follows:  $\theta = 15$  mV,  $\tau = 20$  ms,  $\epsilon_{\text{ext}} = 1.0$  mV,  $\lambda_{\text{ext}} = 500$  Hz,  $\Delta t = 0.00005$  s,  $a_{jk} = 1$ ,  $j \neq k$  and  $a_{jj} = 0$ ,  $V_j(0) = 0$  for all  $j$  and  $t_R = 0$ .

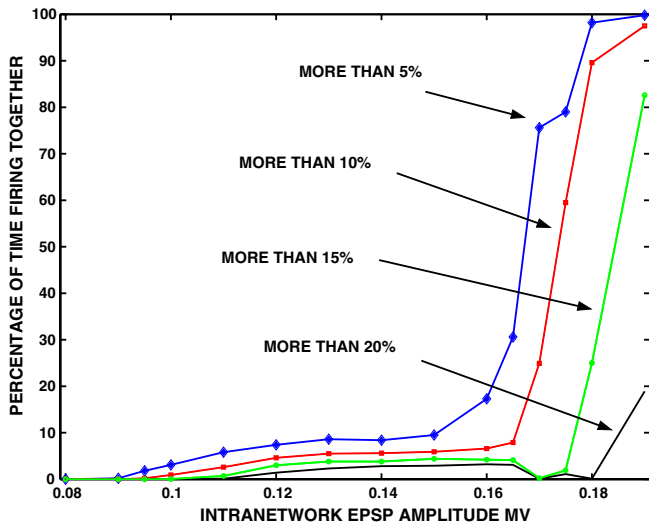


Fig. 8. Indicators of synchronization  $S_5$ ,  $S_{10}$ ,  $S_{15}$  and  $S_{20}$  in an excitatory network of  $n = 100$  neurons as the internal network EPSP amplitude,  $\epsilon_{\text{int}}$ , changes. The blue curve gives the percentage of the time during which more than 5% of cells fired together, if there were any cells firing. Similarly for the red, green and black curves as indicated in the figure. The parameters are as in the caption of the previous figure. (For interpretation of color in this figure legend, the reader is referred to the web version of this article.)

$\theta = 15$  mV,  $\tau = 20$  ms,  $\epsilon_{\text{ext}} = 1.0$  mV,  $\lambda_{\text{ext}} = 500$  Hz,  $\Delta t = 0.000025$  s,  $\epsilon_{\text{int}} = 0.1$  mV,  $a_{jk} = 1$ ,  $j \neq k$  and  $a_{jj} = 0$ ,  $V_j(0)$  uniformly distributed on  $(0, \theta)$  for all  $j$  and  $t_R = 0$ . In Fig. 8 we show plots of the synchronization measures  $S_5$ ,  $S_{10}$ ,  $S_{15}$  and  $S_{20}$  versus the internal EPSP amplitude. It can be seen that for  $\epsilon < 0.08$ , there is asynchronous firing and there seems to be a value,  $\epsilon_c \approx 0.08$ , above which some synchronization starts to occur. As  $\epsilon$  increases beyond  $\epsilon_c$ ,  $S_5$  increases slowly until  $\epsilon$  is about 0.15, whereupon it suddenly increases rapidly to eventually reach 100% at  $\epsilon = 0.19$ . The quantity  $S_{10}$  behaves similarly, but it undergoes a rapid increase at the slightly higher value  $\epsilon = 0.165$ .  $S_{15}$  stays at values less than 5% until  $\epsilon$  is about 0.175 and then suddenly increases.  $S_{20}$  remains at very small values until  $\epsilon > 0.18$ .

Although the amount of synchronization changes continuously for values of  $\epsilon > \epsilon_c$ , there does seem to be an abrupt change in the network firing pattern when  $\epsilon$  reaches about 0.16. However, such behaviour may arise for the particular set of parameters chosen and not be found in general. This issue will be studied in future work. We point out that the analytical approach to estimating neuronal firing rates in the network may perform reasonably well even when there is a small amount of synchronization. This claim is supported by the results in Table 2. Here the remaining parameters are as in the simulations in Fig. 7.

### 3.4. Sparsely connected excitatory networks

Networks in which all elements connect to each other are not without interest, but cortical networks have far less than all-to-all connectivity (Amit and Brunel, 1997b). One

Table 2  
Results and predictions for networks with  $n = 100$

| Internal EPSP size, $\epsilon_{\text{int}}$ | Simulated network frequency | Predicted frequency |
|---|-----------------------------|---------------------|
| 0.05  | 6.3                         | 6.2                 |
| 0.07  | 8.0                         | 6.6                 |
| 0.09  | 12.7                        | 11.9                |

way to reduce the connectivity is not to make all non-diagonal elements of the connection matrix equal to unity but to put  $a_{jk} = 1$  with probability  $p$  where  $0 < p < 1$  when  $j \neq k$  and  $a_{jk} = 0$  otherwise. The analytical method outlined above may still be applied if one uses  $(n - 1)p$  to replace  $n - 1$  in the differential-difference equation (3) for the mean network firing rate. The firing behaviour was found to undergo an abrupt change as  $p$  increased through a critical value. Several trials were performed with the a network of  $n = 500$  using the same parameters as for the previous subsection. With  $p = 0.09$  random firing occurred with probability one and a mean rate of 6.8 Hz, but when  $p = 0.10$  the activity was sometimes random but at others strongly synchronized at very high rates.

### 3.5. An excitatory feed-forward network

Instead of a network where each neuron receives synaptic potentials from a certain number,  $n_{\text{EE}}$ , of other cells, we here consider a network similar to that employed by Van Rossum et al. (2002). The network consists of an input layer of cells which are driven by external sources. Each cell of the input layer connects to a certain number of layer 2 cells. Layer 2 cells in turn connect to a certain number of layer 3 cells and so on. The number of cells is assumed to be  $m$  in each layer and all cells are assumed to have the same time constants  $\tau$  and thresholds  $\theta$ . Each input layer cell receives excitation at rate  $\lambda^{\text{ext}}$  with an EPSP amplitude of  $\epsilon_{\text{ext}}$ . All synapses to internal layer cells involve EPSP's of magnitude  $\epsilon$ .

We will only consider the first layer beyond the input layer, as the same techniques are readily extended to multiple internal layers. Using LIF models for all neurons, we then have for the input layer cells

$$\frac{dU_j}{dt} = -\frac{U_j}{\tau} + \epsilon_{\text{ext}} \frac{dN_j^{\text{ext}}}{dt}, \quad j = 1, \dots, m,$$

where  $N_j^{\text{ext}}$  describes the afferent impulses to the  $j$ th cell and has rate  $\lambda^{\text{ext}}$ . Letting the depolarization of the  $k$ th layer 2 cell be  $V_k$  we have

$$\frac{dV_k}{dt} = -\frac{V_k}{\tau} + \epsilon \sum_{j=1}^m a_{jk} \frac{dN_j}{dt}, \quad k = 1, \dots, m,$$

where  $N_j$  describes the output train of spikes from the  $j$ th input layer cell and  $a_{jk}$  gives the strength of the connection from the latter to the  $k$ th layer 2 cell. All input layer cells fire at the same mean rate  $\lambda$  and assuming there are (any)  $n_{\text{EE}}$  input layer cells connecting with each layer 2 cell, then

the latter fire at rate  $\lambda_2$  which is obtained, assuming cells are initially at rest, as  $\lambda_2 = \frac{1}{F(0)}$  where  $F$  satisfies

$$-\frac{x}{\tau} \frac{dF}{dx} + n_{EE}\lambda[F(x + \epsilon) - F(x)] = -1, \quad x < \theta$$

with the boundary condition  $F(x) = 0, x \geq \theta$ .

An example of spike activity in a simulation of the feed-forward network is shown in Fig. 9. The parameters are as follows:  $m = 100$  (total of 200 neurons),  $n_{EE} = 60$ ,  $\theta = 15$  mV,  $\tau = 0.020$  s,  $\lambda^{\text{ext}} = 500$  Hz,  $\epsilon^{\text{ext}} = 1.25$  mV,  $\epsilon = 1.0$  mV with a timestep of 0.00005 s. We may solve the differential-difference equation for the rate of firing in the second layer, given the rate of spiking in the first layer. Proceeding to do this by solution of the equivalent stochastic differential equation gave a predicted mean layer 2 firing rate of 44.7 Hz per neuron, which compares favourably with the layer 2 network rate of 47.0 Hz per neuron. Note that in this case the distribution of interspike intervals in input layer cells was close to exponential, rendering a Poisson process assumption approximately valid.

### 3.6. A network with excitation and inhibition

Suppose there are  $n_E$  excitatory (type E) and  $n_I$  inhibitory (type I) cells, whose membrane potentials in the absence of synaptic activation satisfy  $\dot{V}_E = f_E(V_E)$  and  $\dot{V}_I = f_I(V_I)$ , respectively. (For the leaky integrate-and-fire model, usually  $f_E(V_E) = -V_E/\tau_E$  where  $\tau_E$  is the membrane time constant; similarly for inhibitory cells.) The postsynaptic potential amplitudes are the (non-negative) quantities  $a_{EE}, a_{IE}, a_{EI}$  and  $a_{II}$ , where the first subscript refers to the presynaptic cell type and the second to the postsynaptic cell type. The corresponding numbers of connections for individual cells are  $n_{EE}, n_{IE}, n_{EI}$  and  $n_{II}$ , respectively. Thus each E-cell receives a total of  $n_{EE} + n_{IE}$  synaptic inputs and an

external input according to the point process  $N_E^{\text{ext}}$  whose rate is  $\lambda_E^{\text{ext}}$  and each I-cell receives  $n_{EI} + n_{II}$  such inputs and an external input according to the point process  $N_I^{\text{ext}}$  whose rate is  $\lambda_I^{\text{ext}}$ . Since each E-cell has effectively the same input, its membrane potential satisfies

$$dV_E = f_E(V_E)dt + a_{EE}dN_{EE}(n_{EE}\lambda_E; t) - a_{IE}dN_{IE}(n_{IE}\lambda_I; t) + \epsilon_E^{\text{ext}}dN_E^{\text{ext}}.$$

For each I-cell,

$$dV_I = f_I(V_I)dt + a_{EI}dN_{EI}(n_{EI}\lambda_E; t) - a_{II}dN_{II}(n_{II}\lambda_I; t) + \epsilon_I^{\text{ext}}dN_I^{\text{ext}}.$$

Here  $N_{EE}, N_{IE}$  are the pooled excitatory and inhibitory input point processes for E-cells and  $N_{EI}, N_{II}$  are the corresponding processes for the I-cells. Letting the thresholds of the two kinds of cell be  $\theta_E$  and  $\theta_I$ , we then have the following result, where now refractory periods are included.

If  $\frac{1}{\lambda_E} + t_{R,E}$  is the mean time interval between spikes in an E-cell and  $\frac{1}{\lambda_I} + t_{R,I}$  is the mean time interval between spikes in an I-cell of the network, then these quantities may be estimated by solving the simultaneous differential-difference equations

$$f_E(v) \frac{dF_E}{dv} + n_{EE}A_E F_E(v + a_{EE}) + n_{IE}A_I F_E(v - a_{IE}) + \lambda_E^{\text{ext}} F(v + \epsilon_E^{\text{ext}}) - (n_{EE}A_E + n_{IE}A_I + \lambda_E^{\text{ext}}) F_E(v) = -1, \quad v < \theta_E,$$

$$f_I(v) \frac{dF_I}{dv} + n_{EI}A_E F_I(v + a_{EI}) + n_{II}A_I F_I(v - a_{II}) + \lambda_I^{\text{ext}} F(v - \epsilon_I^{\text{ext}}) - (n_{EI}A_E + n_{II}A_I + \lambda_I^{\text{ext}}) F_I(v) = -1, \quad v < \theta_I,$$

with boundary conditions  $F_E(v) = 0, v \geq \theta_E, F_I(v) = 0, v \geq \theta_I$  and  $F_E(0) = \frac{1}{\lambda_E}, F_I(0) = \frac{1}{\lambda_I}$ . Here we have put  $A_E = 1 / \left( \frac{1}{\lambda_E} + t_{R,E} \right)$  and  $A_I = 1 / \left( \frac{1}{\lambda_I} + t_{R,I} \right)$ , where  $t_{R,E}$  and  $t_{R,I}$  are the refractory periods of the excitatory and inhibitory cells respectively. In general in the search for such solutions numerically one may insist that  $F_E$  and  $F_I$  vanish for  $v < v_E < 0$  and  $v < v_I < 0$ , respectively, and then let  $v_E$  and  $v_I \rightarrow -\infty$  to ensure that the thresholds for action potentials are attained. The equations for  $F_E$  and  $F_I$  are difficult to solve exactly but may be solved numerically or more easily via simulation of the corresponding stochastic differential equations.

### 3.7. A numerical example

To illustrate that the analytical approach may provide reasonable estimates of network rates when there are inhibitory as well as excitatory elements, we considered a network of 20 excitatory cells and 5 inhibitory cells with the following parameters:  $n_{EE} = 20, n_{EI} = 2, n_{IE} = 2, n_{II} = 0$ , time constants all  $\tau = .020$  s, thresholds all  $\theta = 15$  mV, PSP amplitudes in mV,  $a_{EE} = 0.4, a_{EI} = 0.25, a_{IE} = -0.25$  and  $a_{II} = 0$ . Refractory periods were ignored as the cells fired slowly. The time step in the network simulation was

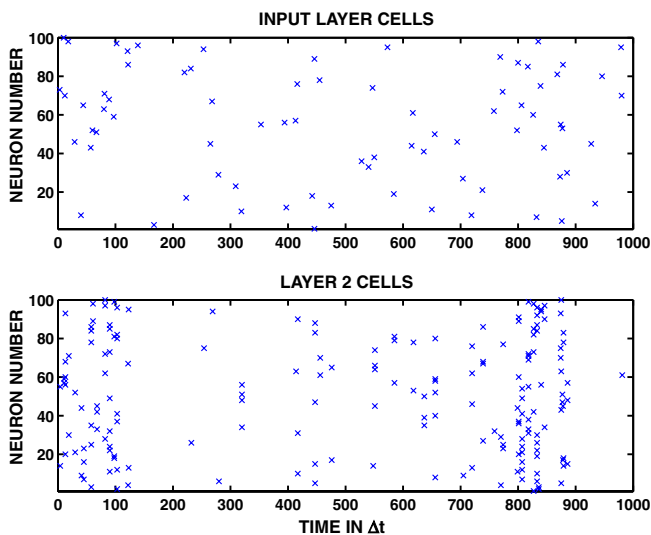


Fig. 9. Spiking activity in the input layer (top) and layer 2 of a feed-forward network with 100 neurons in each layer. For parameter values see text.

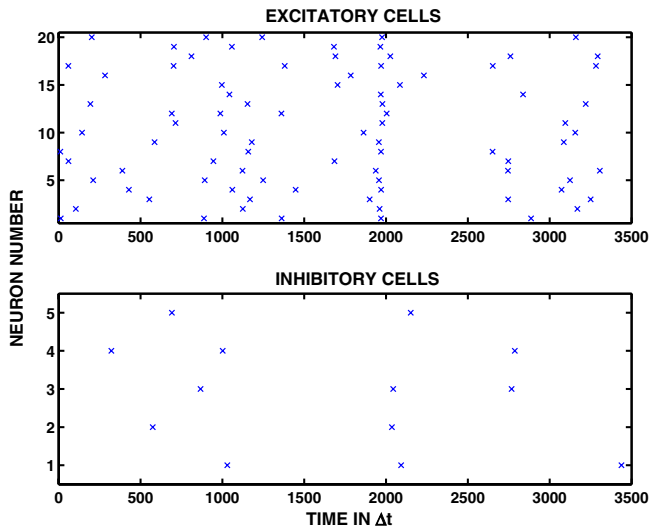


Fig. 10. Spiking activity in the excitatory cells (top) and inhibitory cells in the example given in the text.

$\Delta t = 0.00005$  s. An example of the spike trains obtained is shown in Fig. 10. For 20 such simulations the average spike frequency for the excitatory cells was  $f_E = 22.4$  Hz and that for inhibitory cells was  $f_I = 13.6$  Hz. These rates compare favourably with those obtained by the analytical method (solving the differential-difference equations by simulation techniques) being  $f_E = 24.9$  Hz and  $f_I = 12.2$  Hz. However, other sets of parameters did not lead to such good agreement. This aspect will be addressed in a later publication.

#### 4. Discussion

The cerebral cortex and other brain structures are composed of layers of neurons (and glia) containing distinct kinds of spiny and non-spiny cells. Inputs to both E- and I-cells may have their origins in remote or local cortical areas. We have considered a rudimentary model which could capture a reasonable amount of the biology of real cortex. We focussed attention mainly on networks of excitatory neurons. One objective was to see if an analytical method for estimating firing rates in networks of LIF neuron was accurate when a diffusion approximation is not employed. The totally connected E-network represents the most difficult case to test this approach because there is often a large tendency for such a network to become dominated by synchronously firing groups of neurons. Nevertheless we obtained random sustained firing in such networks with fairly diverse sets of parameter values. When such firing patterns did exist, the analytical approach was often able to predict average neuronal firing rates with considerable accuracy. This was also the case for a simple excitatory feed-forward network and a network composed of excitatory and inhibitory elements.

We also considered several properties of E–E networks, many of which had previously been explored in similar networks (Amit and Brunel, 1997b; Brunel, 2000). Several

kinds of firing pattern were distinguished, including those with silences before and after a period of intense activity. We examined whether firing was synchronous for a given parameter set and investigated how the amount of synchronization depended on the internal EPSP magnitude. The latter was found to have a critical value  $\epsilon_c$ , such that for values of  $\epsilon < \epsilon_c$ , random firing occurred with probability one. We found that as  $\epsilon$  increased beyond  $\epsilon_c$ , the amount of synchronization at first slowly increased and then suddenly rose to large values. We also found network frequency transfer characteristics for various network sizes and found a linear dependence on external afferent frequency over wide ranges of mean input frequency, with non-linear effects at some lower frequencies. In later articles we will explore more complicated models of cortical networks as described in Section 2.

#### Acknowledgements

The author thanks the Max Planck Institute for financial support and Professor Dr. Juergen Jost for his kind hospitality. I am grateful to the referees for many helpful remarks and suggestions.

#### Appendix. Poisson inputs and single neuron frequencies

As there are Poisson afferent inputs in the above model, in order to simulate the activity in the above network, and also to simulate single neuron activity, it is required to obtain accurate sequences of event times in Poisson processes. It is found that if the sequences are not accurate then the network results can be very misleading. There are two ways to generate such sequences, both of which utilize random variables with a uniform distribution on the unit interval – designated as  $U(0, 1)$  random variables. Let us assume that the frequency of events is  $\lambda$ . In the first method, which we call the direct method, the probability integral transformation (Tuckwell, 1995) is used whereby if  $U_k$ ,  $k = 1, 2, \dots$ , is a sequence of  $U(0, 1)$  random variables which are independent, then  $X_k = -\frac{1}{\lambda} \log(1 - U_k)$ ,  $k = 1, 2, \dots$ , is a sequence of random variables which are exponentially distributed with means  $\frac{1}{\lambda}$ . This implies that the sequence  $T_n = \sum_{k=1}^n X_k$ ,  $n = 1, 2, \dots$  is a sequence of event times in a Poisson process of rate  $\lambda$ . With this method there is little room for error. In the second method, we use the fact that in a Poisson process, the probability of an event in a small time interval  $(t, t + \Delta t]$  is close to  $\lambda \Delta t$ . Thus, if a generated  $U(0, 1)$  variable is less than  $\lambda \Delta t$ , an event is assumed to have occurred, and no event otherwise. We used both methods to determine the firing frequency of an LIF neuron in a case where an exact result is available (Tuckwell, 1975). Here the stochastic equation is

$$dV = -\frac{V}{\tau} dt + \epsilon dN(\lambda; t),$$

so that EPSPs of amplitude  $\epsilon$  arrive with rate  $\lambda$ . An input frequency of 1 per time constant and an EPSP amplitude

one half of the threshold, gives an expected time for the depolarization to reach firing threshold from rest of

$$E[T] = 2 + \frac{1}{1 - \ln 2}.$$

A comparison of the results obtained by the two methods described above is shown in the following table:

#### Comparison of simulation methods

| Method of solution                 | $E[T]$ |
|------------------------------------|--------|
| Exact analytic result              | 5.259  |
| Direct method                      | 5.26   |
| Second method, $\Delta t = 0.001$  | 5.35   |
| Second method, $\Delta t = 0.0005$ | 5.30   |

It can be seen in this example that the direct method is the most accurate, as is expected as there is no approximation involved. The second method is more convenient but can be inaccurate unless a suitably small step size is used.

#### References

- Abbott, L.F., Van Vreeswijk, C., 1993. Asynchronous states in networks of pulse-coupled oscillators. *Phys. Rev. E* 48, 1483–1490.
- Abeles, M., 1991. *Corticonics*. Cambridge University Press, New York.
- Amit, D., 1989. *Modeling Brain Function*. Cambridge University Press, Cambridge.
- Amit, D., Brunel, N., 1997a. Model of global spontaneous activity and local structured activity during delay periods in the cerebral cortex. *Cerebral Cortex* 7, 237–252.
- Amit, D., Brunel, N., 1997b. Dynamics of a recurrent network of spiking neurons before and following learning. *Network* 8, 373–404.
- Axmacher, N., Mormann, F., Fernandez, G., Elger, C., Fell, J., 2006. Memory formation by neuronal synchronization. *Brain Res. Rev.* 52, 170–182.
- Bazhenov, M., Rulkov, N.F., Fellous, J.-M., Timofeev, I., 2005. Role of networks in shaping spike timing reliability. *Phys. Rev. E* 72, 041903.
- Beurle, R.L., 1956. Properties of a mass of cells capable of regenerating pulses. *Philos. Trans. R. Soc. A240*, 55–97.
- Binzegger, T., Douglas, R.J., Martin, K.A.C., 2005. Cortical architecture. *Lect. Notes Comput. Sci.* 3704, 15–28.
- Bresloff, P.C., Coombes, S., 1998. Spike train dynamics underlying pattern formation in integrate-and-fire oscillator networks. *Phys. Rev. Lett.* 81, 2384–2387.
- Brunel, N., 2000. Dynamics of networks of randomly connected excitatory and inhibitory spiking neurons. *J. Physiol. (Paris)* 94, 445–463.
- Brunel, N., 2003. Dynamics and plasticity of stimulus-selective persistent activity in cortical network models. *Cerebral Cortex* 13, 1151–1161.
- Brunel, N., Hakim, V., 1999. Fast global oscillations in networks of integrate-and-fire neurons with low firing rates. *Neural Comput.* 11, 1621–1671.
- Brunel, N., Hansel, D., 2006. How noise affects the synchronization properties of recurrent networks of inhibitory neurons. *Neural Comput.* 18, 1066–1110.
- Brunel, N., Chance, F.S., Fourcaud, N., Abbott, L.F., 2001. Effects of synaptic noise and filtering on the frequency response of spiking neurons. *Phys. Rev. Lett.* 86, 2186–2189.
- Bush, P.C., Sejnowski, T.J., 1995. Models of cortical networks. In: Gutnick, M.L., Mody, I. (Eds.), *The Cortical Neuron*. Oxford University Press, Oxford (Chapter 12).
- Deco, G., Rolls, E.T., 2005. Synaptic and spiking dynamics underlying reward reversal in the orbitofrontal cortex. *Cerebral Cortex* 15, 15–30.
- Deng, Y., Ding, M., Feng, J., 2004. Synchronization in stochastic coupled systems: theoretical results. *J. Phys. A* 37, 2163–2173.
- Destexhe, A., Paré, D., 1999. Impact of network activity on the integrative properties of neocortical pyramidal neurons in vivo. *J. Neurophysiol.* 81, 1531–1547.
- Destexhe, A., Rudolph, M., Fellous, J.-M., Sejnowski, T.J., 2001. Fluctuating synaptic conductances recreate in vivo-like activity in neocortical neurons. *Neuroscience* 107, 13–24.
- Douglas, R.J., Martin, K.A.C., 2004. Neuronal circuits of the neocortex. *Ann. Rev. Neurosci.* 27, 419–451.
- Gerstner, W., 2000. Population dynamics of spiking neurons: fast transients, asynchronous states and locking. *Neural Comput.* 12, 43–89.
- Gerstner, W., Kistler, W.M., 2002. *Spiking Neuron Models*. Cambridge University Press, Cambridge.
- Grillner, S., Markram, H., De Schutter, E., Silberberg, G., LeBeau, F.E.N., 2005. Microcircuits in action – from CPGs to neocortex. *Trends Neurosci.* 28, 525–533.
- Hausler, S., Maass, W., 2006. A statistical analysis of information-processing of lamina-specific cortical microcircuit models. *Cerebral Cortex*, available online.
- Hansel, D., Mato, G., 2003. Asynchronous states and the emergence of synchrony in large networks of interacting excitatory and inhibitory neurons. *Neural Comput.* 15, 1–56.
- Hebb, D.O., 1949. *The Organization of Behavior*. Wiley, New York.
- Hilgetag, C.C., Barbas, H., 2006. Role of mechanical factors in the morphology of the primate cerebral cortex. *PLoS Comput. Biol.* 2, e22.
- Hopfield, J.J., 1982. Neural networks and physical systems with emergent collective computational abilities. *PNAS* 79, 2554–2558.
- Knight, B.W., 1972. Dynamics of encoding in a population of neurons. *J. Gen. Physiol.* 59, 734–766.
- Konig, P., 1994. A method for the quantification of synchrony and oscillatory properties of neuronal activity. *J. Neurosci. Methods* 54, 31–37.
- Konig, P., Engel, A.K., Singer, W., 1996a. Relation between oscillatory activity and long-range synchronization in cat visual cortex. *PNAS* 92, 290–294.
- Konig, P., Engel, A.K., Singer, W., 1996b. Integrator or coincidence detector? The role of the cortical neuron revisited. *Trends Neurosci.* 19, 130–137.
- Liley, D.T.J., Alexander, D.M., Wright, J.J., Aldous, M.D., 1999. Alpha-rhythm emerges from large-scale networks of realistically coupled multicompartamental model cortical neurons. *Network* 10, 79–92.
- McCormick, D.A., Connors, B.W., Lighthall, J.W., Prince, D.A., 1985. Comparative electrophysiology of pyramidal and sparsely spiny neurons of the neocortex. *J. Neurophysiol.* 54, 782–806.
- Neltner, L., Hansel, D., Mato, G., Meunier, C., 2000. Synchrony in heterogeneous networks of spiking neurons. *Neural Comput.* 12, 1607–1641.
- Perez-Orive, J., Bazhenov, M., Laurent, G., 2004. Intrinsic and circuit properties favor coincidence detection for decoding oscillatory input. *J. Neurosci.* 24, 6037–6047.
- Rulkov, N.F., Timofeev, I., Bazhenov, M., 2004. Oscillations in large scale cortical networks: map-based model. *J. Comput. Neurosci.* 17, 203–223.
- Samonds, J.M., Bonds, A.B., 2004. Real-time visualization of neural synchrony for identifying coordinated cell assemblies. *J. Neurosci. Methods* 139, 51–60.
- Sherrington, C.S., 1906. *The Integrative Action of the Nervous System*. Cambridge University Press, Cambridge.
- Singer, W., 1993. Synchronization of cortical activity and its putative role in information processing and learning. *Ann. Rev. Physiol.* 55, 349–374.
- Singer, W., 1999. Neural synchrony: a versatile code for the definition of relations? *Neuron* 24, 49–65.
- Somogyi, P., Tamas, G., Lujan, R., Buhl, E.H., 1998. Salient features of synaptic organization in the cerebral cortex. *Brain Res. Rev.* 26, 113–135.

- Tiesinga, P.H.E., José, J.V., 2000. Robust gamma oscillations in networks of inhibitory hippocampal neurons. *Network* 11, 1–23.
- Tuckwell, H.C., 1975. Determination of the interspike times of neurons receiving randomly arriving postsynaptic potentials. *Biol. Cybern.* 18, 225–237.
- Tuckwell, H.C., 1995. *Elementary Applications of Probability Theory: with an Introduction to Stochastic Differential Equations*. Chapman and Hall, London.
- Tuckwell, H.C., 1998. Continuum models in neurobiology and information processing. *BioSystems* 48, 223–228.
- Tuckwell, H.C., Cope, D.K., 1980. Accuracy of neuronal interspike times calculated from a diffusion approximation. *J. Theor. Biol.* 83, 377–387.
- Tuckwell, H.C., Feng, J.-F., 2006. Estimation of spike train statistics in spontaneously active biological neural networks. In: Feng, J.-F., Jost, J., Qian, M. (Eds.), *Network: From Biology to Theory*. Springer, Berlin.
- Tuckwell, H.C., Miura, R.M., 1978. A mathematical model for spreading cortical depression. *Biophys. J.* 23, 257–276.
- Van Rossum, M.C.W., Turrigiano, G.G., Nelson, S.B., 2002. Fast propagation of firing rates through layered networks of noisy neurons. *J. Neurosci.* 22, 1956–1966.
- Van Vreeswijk, C., Abbott, L.F., 1993. Self sustained firing in populations of integrate-and-fire neurons. *SIAM J. Appl. Math.* 83, 253–264.